Published in final edited form as:
Dev Cell. 2011 October 18; 21(4): 627–641. doi:10.1016/j.devcel.2011.08.005.

A Conserved Pbx-Wnt-p63-Irf6 Regulatory Module Controls Face Morphogenesis by Promoting Epithelial Apoptosis

Elisabetta Ferretti[1], **Bingsi Li**[1], **Rediet Zewdu**[1], **Victoria Wells**[1], **Jean M. Hebert**[2], **Courtney Karner**[3], **Matthew J. Anderson**[4], **Trevor Williams**[5], **Jill Dixon**[6], **Michael J. Dixon**[6], **Michael J. Depew**[7], and **Licia Selleri**[1]

[1]Dept. of Cell and Developmental Biology, Weill Medical College of Cornell University, New York, NY

[2]Depts. of Neuroscience & Genetics, Albert Einstein College of Medicine, New York, NY

[3]Depts. of Internal Medicine & Molecular Biology, University of Texas, Southwestern Medical Center, Dallas, TX

[4]Genetics of Vertebrate Development Section, National Cancer Institute, Frederick, MD

[5]Depts. of Craniofacial Biology & Cell and Developmental Biology, University of Colorado Denver

[6]Faculty of Medical and Human Sciences, Manchester Academic Health Sciences Center, University of Manchester, Manchester, UK

[7]Dept. of Craniofacial Development, King's College London, London, UK

Abstract

Morphogenesis of mammalian facial processes requires coordination of cellular proliferation, migration, and apoptosis to develop intricate features. Cleft lip and/or palate (CL/P), the most frequent human craniofacial birth defect, can be caused by perturbation of any of these programs. Mutations of *WNT*, *P63*, and *IRF6* yield CL/P in humans and mice; however, how these genes are regulated remains elusive. We generated mouse lines lacking *Pbx* genes in cephalic ectoderm and demonstrated that they exhibit fully penetrant CL/P and perturbed Wnt signalling. We also characterized a midfacial regulatory element that Pbx proteins bind in order to control the expression of *Wnt9b-Wnt3*, which in turn regulate *p63*. Altogether, we establish a Pbx-dependent Wnt-p63-Irf6 regulatory module in midfacial ectoderm that is conserved within mammals. Dysregulation of this network leads to localized suppression of midfacial apoptosis and CL/P. Ectopic *Wnt* ectodermal expression in *Pbx* mutants rescues the clefting, opening avenues for tissue repair.

Keywords

Face; Ectoderm; Lambdoidal Junction; Pbx; Wnt; p63; Irf6; Wnt midfacial enhancer; CL/P; Mouse

Correspondence to: Licia Selleri.

Introduction

Facial appearance provides immediate cues that facilitate direct interpersonal communication among humans. In mammals, morphogenesis of the face requires precise coordination of cellular programs including proliferation, migration, growth, differentiation, and apoptosis (Cox et al., 2004). As mice and humans share similar craniofacial morphology during development (Gritli-Linde, 2008; Tamarine and Boyde, 1977), the mouse offers a suitable model to study these processes. Murine facial morphogenesis is heralded by the appearance of the frontonasal process (fnp) and paired maxillary processes (mxp), which arise from branchial arch (BA) 1 at embryonic day E9.5 (4^{th} week of gestation in humans). By E10.5 (late 4^{th} week in humans), the fnp divides into paired medial nasal process (mnp) and lateral nasal process (lnp). Development of the midface, including the upper lip, primary palate, alae of the nose, and nostrils involves adequate growth and fusion of the mxp, mnp, and lnp (Depew and Compagnucci, 2008; Gritli-Linde, 2008).

With an incidence of 1 in 700 live births, clefting of the lip and palate is the most common human craniofacial birth abnormality (Dixon et al., 2011). Cleft lip, with or without cleft palate (CL/P), and isolated cleft palate (CPO) are regarded as being both developmentally and genetically distinct. The majority of CL/P are nonsyndromic and their transmission is non-mendelian. CL/P results from the failure of the mxp to fuse with the mnp, while CPO from the lack of fusion of the two palatine shelves along the midline (Cox et al., 2004). Mutations of members of the *WNT*, *FGF*, and *FGFR* families of signaling molecules and in the genes encoding the transcription factors (TFs) IRF6, P63, and AP2A result in forms of CL/P in humans (Kondo et al., 2002; Milunsky et al., 2008; Niemann et al., 2004; Riley et al., 2007; Rinne et al., 2007).

In the mouse, the three-way seam at which the mxp, mnp, and lnp coalesce, named lambdoidal junction (λ) (Depew and Compagnucci, 2008; Tamarine and Boyde, 1977), is characterized by marked expression of *Wnt* and *Bmp* genes, as well as *Irf6* and *p63*. Mutations of these genes lead to CL/P in mice as well as humans, thus providing animal models to study human clefting (Brugmann et al., 2007; Carroll et al., 2005; Ingraham et al., 2006; Lan et al., 2007; Liu et al., 2005; Reid et al., 2011; Song et al., 2009; Thomason et al., 2008; Wang et al., 2011). Moreover, the spontaneous mouse mutant *A/WySv*, which exhibits CL/P, is caused by mutations of the *cfl1* locus, which maps to mouse chromosome 11 within a region syntenic to human 17q21. The latter is associated with human orofacial clefting (Juriloff et al., 2006). Mutations of *cfl1*, which encompasses *Wnt3* and *Wnt9b*, do not complement the CL/P phenotype of *Wnt9b*$^{-/-}$ mice, indicating that *cfl1* and *Wnt9b* are within the same locus (Carroll et al., 2005; Juriloff et al., 2006). Notably, Wnt/β–catenin signaling via TCF-dependent transcription (hereafter referred to as Wnt signaling) is strong at the murine λ (Lan et al., 2007).

Here, we report that *Pbx* genes (*Pbx1-2-3*), which encode TALE homeodomain-containing TFs (Moens and Selleri, 2006), are highly expressed at the λ during mouse facial development. Pbx1-2-3 proteins, which are generally regarded as Hox ancillary factors that increase Hox DNA-binding specificity (Tumpel et al., 2009), are required for mouse organogenesis (Selleri et al., 2001; Vitobello et al., 2011) and skeletal development (Capellini et al., 2006 and 2010). By generating mice deficient for multiple *Pbx* genes, we demonstrated that compound *Pbx* loss in the surface cephalic ectoderm (SCE) results in craniofacial abnormalities and fully penetrant CL/P. In this model for CL/P we established that, by binding to a *Wnt9b-Wnt3* midfacial regulatory element (RE), *Pbx* proteins directly regulate Wnt signaling, which in turn controls *p63* at λ. We proved the essential requirement of Pbx-directed Wnt signaling for midfacial morphogenesis by complete rescue of the CL phenotype in *Pbx* mutants via *Wnt* ectopic expression in SCE. Altogether, we characterized

a Pbx-dependent Wnt-p63-Irf6 regulatory module at λ, which is conserved only within mammals. Disruption of the delineated module leads to localized suppression of apoptosis at λ and yields midfacial clefting.

Results

Pbx1-2-3 homeoproteins are required for midface morphogenesis and their compound loss causes fully penetrant CL/P

Pbx1-2-3 homeoproteins are required for organogenesis and skeletogenesis (Cappellini et al., 2006 and 2010; Selleri et al., 2001; Vitobello et al., 2011). Although the products of murine *Pbx* genes are traditionally considered as Hox cofactors, during development they are present in domains broader than those of Hox proteins, particularly in the head. At E8.5–9.0, *Pbx* transcripts were expressed within the fnp and BA1, as well as in E9.0 SCE and mesenchyme. By E10.5, *Pbx1-2-3* expression levels increased in the epithelium of the mxp, mnp, and lnp (Figure 1A–1C). Use of antibodies (Abs) specific for Pbx1, Pbx2, Pbx3, and for their dimerization partners Meis and Prep1 (Ferretti el al., 2000; Moens and Selleri, 2006), confirmed higher TALE protein levels in the epithelium *versus* the mesenchyme (Figure 1D–1G; Figure S1A–S1F). Notably, qRT-PCR assays on RNA extracted from mxp, mnp, and lnp revealed that, among *Pbx* genes, *Pbx1* expression is highest (Figure S1G). To uncover *Pbx* roles during morphogenesis of the face, a “Hox-less” domain in the early embryo (Creuzet et al., 2005; Figure S2A–2B), we examined craniofacial phenotypes of *Pbx* compound mutants, by intercrossing $Pbx1^{+/-}$, $Pbx2^{+/-}$, and $Pbx3^{+/-}$ mice (Rhee et al., 2004; Selleri et al., 2001 and 2004). We observed that, among the *Pbx* compound mutant genotypes obtained (table S1), only $Pbx1^{-/-};Pbx2^{+/-}$ (n=42; hereafter *Pbx1/2* mutants) and $Pbx1^{-/-};Pbx3^{+/-}$ (n=23; hereafter *Pbx1/3* mutants) embryos showed fully penetrant bilateral or unilateral CL/P and jaw hypoplasia, while $Pbx1^{+/-};Pbx2^{+/-};Pbx3^{+/-}$ mutants died at birth with CPO (Figure 2A–2D; Figure S3A–S3D). These results highlighted the preeminent role of *Pbx1* in midfacial morphogenesis and the collaborative functions of *Pbx2* and *Pbx3* in domains of co-expression. Our findings revealed Hox-independent roles for Pbx homeoproteins in midface morphogenesis.

Pbx1 SCE-specific inactivation on a *Pbx2*- or *Pbx3*-deficient background results in midfacial clefting

To address tissue-specific Pbx requirements, we conditionally inactivated *Pbx1* (Koss et al., under review), on a *Pbx2*- (Selleri et al., 2004) or *Pbx3*- (Rhee et al., 2004) deficient background, in either SCE or cranial neural crest (CNC)-derived mesenchyme migrating into the fnp (Noden and Trainor, 2005). We used *Foxg1*-Cre (Hebert and McConnell, 2000) or *Crect*-Cre (Reid et al., 2011) deleter strains for SCE-specific inactivation, and the *Wnt1-Cre* line (Rowitch et al., 1999) for mesenchyme-specific inactivation. *Pbx1* loss from *Foxg1*-positive (and *Crect*-positive) domains on a *Pbx2*- or *Pbx3*-deficient background resulted in CL/P (Figure 2E–2F; also Figure 8J–8K below), recapitulating *Pbx1/2* and *Pbx1/3* compound mutant phenotypes.

Skeletal preparations of $Pbx1^{flox/flox};Pbx2^{+/-};Foxg1^{Cre/+}$ mutants, which die shortly after birth, showed abnormalities in the nasal capsule (nc), maxillary palatal and palatine process, and absence of pre-maxillary process (Figure 2I and 2J). In contrast, *Pbx1* inactivation in *Wnt1*-positive CNC on a *Pbx2*-deficient background, which also resulted in postnatal lethality, did not yield CL, but resulted in CPO (Figure 2G and 2H; 2K and 2L). Consistent with previous findings, we detected *Cre* recombination by X-gal staining in midfacial SCE of $Foxg1^{Cre/+};R26R\text{-}LacZ$ embryos (Soriano, 1999) and in mesenchyme of $Wnt1^{Cre/+};R26R\text{-}LacZ$ embryos already at E9.5 (Figure S3E–S3F). We confirmed efficient *Pbx1* Cre-mediated excision in midfacial SCE and mesenchyme of *Pbx1* conditional mutants

versus littermates at E 13.5 (Figure 2M–2P). However, only SCE-specific deletion of *Pbx1* on a *Pbx2*- or *Pbx3*-deficient background yielded CL/P.

Pbx genes control *Wnt9b-Wnt3*, which in turn act upstream of *Fgf8* at λ

Wnt, *Lrp* and *Fzd* family members, and their effectors *Tcf4*/*Lef1*, play major roles in head formation and are expressed in midfacial SCE, resulting in active Wnt signaling at λ (Brugmann et al., 2007; Fossat et al., 2011; Lan et al., 2006; Reid et al 2011; Song et al., 2009; Wang et al., 2011). *Tcf4*;*Lef1* compound deletions yield facial phenotypes, including widened midface (Brugmann et al., 2007), which resembles that of *Pbx* mutants, albeit lacking clefting (Figure 2A–2D; Figure S3A). Furthermore, the *clf1* spontaneous mouse mutation maps to a region encompassing *Wnt9b-Wnt3*, and some $Wnt9b^{-/-}$ embryos exhibit CL/P (Carroll et al., 2005; Juriloff et al., 2006). Lastly, nonsense mutations in *WNT3* yield human CL/P (Niemann et al., 2004). Thus, we tested whether *Wnt9b* and *Wnt3* expression is perturbed in *Pbx* compound mutant midface. Both transcripts were present at low levels in SCE of E9.25 controls, while they were absent from SCE of *Pbx1/2* mutants (Figure S4A–S4D). At later stages, while higher levels of *Wnt9b* and *Wnt3* transcripts were present at λ in controls, they were absent from SCE and λ of *Pbx1/2* mutants (Figure 3A–3D; Figure S4). Given previous findings that both Wnt9b and Wnt3 act through Wnt canonical signaling (Carroll et al. 2005; van Amerongen and Nusse, 2009), we evaluated Wnt canonical activity in the midface of *Pbx* compound mutants using Wnt reporter (*BAT-gal*) mice (Maretto et al., 2003). We demonstrated that Wnt activity is detectable in SCE of E9.5 controls, while it is markedly reduced in *Pbx* mutants (Figure S4E–S4F'). Similarly, at later stages, Wnt activity was strong in SCE and λ of controls, while it was absent from this connecting center in *Pbx* mutants (Figure 3E–3H'; Figure S4).

Given the role of *Fgf8* as a target of Wnt/β-catenin in head morphogenesis (Paek et al., 2011; Reid et al., 2011; Wang et al., 2011), we analyzed *Fgf8* expression in Pbx compound and $Wnt9b^{-/-}$ mutants. At E9.25-E9.5, *Fgf8* showed similar expression in midfacial epithelial domains of control and mutant embryos (Figure 3I–3J'; 3Q–3R'). However, from E10.5–E11.5, *Fgf8* was absent at λ of *Pbx* compound and $Wnt9b^{-/-}$ mutants (Figure 3K–3N; 3S and 3T). By E11.0, *Fgf8* and *Fgf9* were similarly expressed at λ and in the oral epithelium of controls (Figure 3S and 3U; Figure S5A–S5E'). However, while *Fgf8* was lost from these domains in *Pbx1/2*, *Pbx1/3*, and $Wnt9b^{-/-}$ mutants, *Fgf9* expression was maintained (Figure 3O and 3P; 3U and 3V; Figure S5), indicating that mutant λ is not devoid of gene expression and that select genetic pathways are similarly perturbed in *Pbx* and *Wnt9b* mutants. Additionally, we found that *Pbx1* was expressed at similar levels at the λ of $Wnt9b^{-/-}$ and controls (Figure 3W and 3X). Furthermore, *Wnt9b* SCE-specific inactivation, using *Foxg1-Cre* mice, resulted in CL/P that recapitulated that of $Wnt9^{-/-}$ and $Pbx1^{flox/flox};Pbx2^{+/-};Foxg1^{Cre/+}$ embryos (Figure 4A). These findings emphasized that CL/P in both *Pbx1/2* and *Wnt9b* mutants has a common genetic basis. To order *Pbx1*, *Wnt9b*, and *Fgf8* within a genetic cascade controlling midfacial morphogenesis, given the early lethality of *Fgf8* mutants, we examined *Wnt9b* expression in *Fgf8* hypomorphic embryos (Meyer et al., 1998). *Wnt9b* showed identical patterns at the λ and oral epithelium of controls and *Fgf8* hypomorphs (Figure S5G–S5J). Moreover, we observed that loss of even one *Pbx1* allele on a $Wnt9b^{-/-}$ background increased the incidence of CL compared to $Wnt9b^{-/-}$ single mutant embryos from 59% to 100% (Figure 4B), demonstrating a strong genetic interaction between *Pbx1* and *Wnt9b* in midfacial morphogenesis. Altogether, these results suggested that *Fgf8* does not act upstream of *Wnt9b* and that *Wnt9b* does not control *Pbx1* expression. In light of these findings and the observation that both *Wnt9b* and *Fgf8* are down-regulated or absent at the *Pbx* mutant λ, we established a genetic cascade wherein *Pbx* genes control *Wnt9b-Wnt3* which, in turn, act upstream of *Fgf8* in midface morphogenesis.

Additionally, to assess whether abnormal migration of CNC (Noden and Trainor, 2005) into the facial processes contributes to CL/P in *Pbx* mutants, we analyzed *AP2α*-expression in *Pbx1/2* mutant *versus* control embryos and found it unperturbed (Figure S5K and S5L). Lastly, to verify the integrity of the olfactory placode and SCE in E9.5–10.5 *Pbx1/2* mutants, we demonstrated that the expression of *Raldh3* and *Foxg1*, respectively, was unchanged in *Pbx1/2* mutants *versus* controls (Figure S5M–S5P'). Altogether, these results indicated that in *Pbx1/2* mutants early CNC migration into the facial processes is generally unperturbed and the olfactory placode and SCE are grossly unaffected.

Recruitment of Pbx-Prep(Meis) complexes to a *Wnt9b-Wnt3* midfacial regulatory element transactivates *Wnt* in mouse embryonic midface

Wnt9b and *Wnt3* are oriented head-to-head on murine chromosome 11 and share a 24 kb intergenic region (IR) (Katoh, 2005), which is evolutionarily conserved across vertebrates, except for fish (Figure 5A and 5B). To test whether Pbx proteins control *Wnt9b-Wnt3* expression via binding to the IR, we performed chromatin immunoprecipitation (ChIP) analyses on the IR segments with the highest sequence conservation (W0–W5), containing putative *Pbx-Prep(Meis)* binding sites. ChIP-qPCR on chromatin derived from midfacial processes with Pbx, Meis/Prep, and Hox Abs showed Pbx-Prep1 enrichment on W1 and W3, but not on other elements (Figure 5C and 5D; Figure S6A and S6B). These findings established that the *Wnt9b-Wnt3* IR is a direct target of Pbx binding *in vivo*, containing potential Pbx (TGAT) and Pbx1-Prep(Meis) (PM) binding sites (TGACAG) (Ferretti et al., 2000), which are conserved within amniotes (Figure 5B).

Furthermore, EMSA with *in vitro* translated proteins and midfacial nuclear extracts (NE) and the W3 oligonucleotide showed slower migrating bands comprising Pbx1a-Prep1, Pbx2-Prep1, Pbx3-Prep1 (upper complex; UC) and Pbx1b-Prep1 (lower complex; LC), indicating that W3-binding Pbx-Prep1 and Pbx-Meis heterodimers were present in facial processes. Additionally, competition of DNA-binding with specific Abs revealed that the formation of both UC and LC was inhibited by Prep1 Ab, and partially by PanPbx, Pbx2, Pbx1b, and Pbx3 Abs, but not by IgG (Figure 5E and S6E). Lastly, Pbx DNA-binding specificity was confirmed by competition with unlabeled wild type (wt) oligonucleotides and lack of competition by mutated oligonucleotides (Figure S6F). These data corroborated binding of the Pbx-Prep(Meis) complexes to the *Wnt9b-Wnt3* IR also *in vitro* via a typical PM motif within the IR.

Subsequently, we generated transgenic mouse embryos containing concatamerized DNA fragments spanning 1700 base pairs (bp) (Tg1) and 400 bp (Tg3) of W3 (Experimental Procedures) to test the activity of the W3 RE for *Wnt9b-Wnt3* expression at λ (Figure 5F). The majority of embryos carrying *Tg1* and *Tg3* expressed *LacZ* in midfacial domains that were superimposable on those exhibiting Wnt activity in BAT-gal embryos (Table S2). To establish whether the PM motif was required for W3 RE activity *in vivo*, we introduced point mutations within the binding site inside the 400bp fragment of the *Tg3* transgene (*Tg3Mut*) that were identical to those introduced in oligonucleotide W3m12 used in EMSA (Figure S6C). Out of 17 PCR-positive *Tg3Mut* embryos, only 1 showed any, albeit very weak, midfacial *LacZ* expression (Figure 5F). These findings established that the PM binding element within the W3 midfacial RE is required for *Wnt9b-Wnt3* transcriptional activity *in vivo*.

Pbx1 SCE-specific inactivation on a Pbx2-deficient background causes abnormal cellular morphology at λ, perturbed *p63* expression, and localized suppression of apoptosis

CL became evident in *Pbx* mutants by E11.5, when the lnp and mnp fused abnormally, with persistence of an abnormal "bridge" connecting their posterior aspects to the anterior mxp

(Figure 6A and 6B). To identify the cell type forming this "bridge" and to assess whether it was SCE-derived, we performed fate mapping experiments crossing *R26R-LacZ* reporter mice to the *Pbx1*$^{+/flox}$;*Pbx2*$^{+/-}$;*Foxg1*$^{Cre/+}$ line. We found that in control embryos LacZ-positive SCE contributed to the epithelial seams, which fused to be progressively substituted by LacZ-negative mesenchyme at the λ (Figure 6C). In contrast, in *Pbx1*$^{flox/flox}$;*Pbx2*$^{+/-}$;*Foxg1*$^{Cre/+}$;*R26R-LacZ* mutants the epithelial seams did not fuse leaving a "bridge" comprising LacZ-positive cells (Figure 6D). These findings indicated that λ epithelial seams in *Pbx* mutants retain epithelial characteristics. Additionally, we showed that while in controls the epithelial seams fuse and cells therein exhibit barely detectable E-cadherin levels, in *Pbx1*$^{flox/flox}$;*Pbx2*$^{-/-}$;*Foxg1*$^{Cre/+}$ mutants they do not fuse and cells within the aberrant "bridge" are E-cadherin-positive (Figure 6E and 6F).

To understand the molecular mechanisms underlying epithelial removal at λ, we analyzed expression of the epithelial marker *p63*, since mutations in both human and murine *P63* cause CL/P (Rinne et al., 2007; Thomason et al., 2008). We found down-regulation of *p63* at λ of both *Pbx1/2* and *Wnt9b*$^{-/-}$ mutants (Figure 6G–6J), indicating an upstream genetic role of *Pbx* genes on *p63* via *Wnt9b*. At λ, multiple cellular processes, including apoptosis, mediate removal of epithelial cells at the seams (Cox, 2004; Jiang et al., 2006; Song et al., 2009). Apoptosis ensures that adequate cell numbers are removed from the tips of the epithelial seams to facilitate adhesion of the converging midfacial processes and occurs before and during their fusion in control embryos (Figure 6K, 6M; Figure S7A and 7B). We detected apoptotic cells at the tip of the epithelial seams in controls, but not in the corresponding domains of *Pbx* and *p63* mutant embryos (Yang et al. 1999) (Figure 6L–6N; Figure S7A and S7B), revealing localized suppression of apoptosis at λ of both mutants. These results indicated that the epithelial seams are removed by apoptosis in normal morphogenesis of the upper lip.

To assess whether proliferation defects may concomitantly mediate the *Pbx* mutant CL/P phenotype, we examined proliferation rates of both epithelial and mesenchymal cells in control and *Pbx* compound mutant λ at different gestational days. We did not find significant differences in proliferation rates of epithelial and mesenchymal cells between *Pbx* compound mutants and controls (Figure S7C and S7D), highlighting the importance of localized loss of apoptosis in the genesis of CL/P in these mutants.

Interestingly, *p63* expression and Wnt activity were superimposable at λ in control embryos, and similarly down-regulated in *Pbx* and *Wnt9b*$^{-/-}$ mutants (compare Figure 6G-5J to Figure 3E–3H'). Accordingly, we tested whether *p63* was a target of Wnt, by searching for potential Lef-Tcf binding sites within conserved regions of the *p63* gene. Four putative Lef-Tcf binding sites were found within regions named A to D, inside highly conserved *p63* introns (Figure 7A, 7B). ChIP-qPCR using a Lef1 Ab on E10.5 facial process chromatin showed *p63* enrichment only on region A (*p63A*) relative to IgG control (Figure 7C), demonstrating specific binding *in vivo*. Within region A, we identified a Lef-Tcf binding site (ATCAAAG) that is conserved within amniotes (Figure 7B). EMSA on NE from wt facial processes with an oligonucleotide spanning the *p63A* region over the putative Lef-Tcf binding site (Figure 7D), showed several complexes bound to the *p63A* oligonucleotide (Figure 7E). However, only one complex was specifically competed by the addition of Lef1 Ab. Competition of Lef1 DNA-binding specificity to the *p63A* oligonucleotide was confirmed with molar excess of wt cold oligonucleotide, but not with a mutated oligonucleotide (*p63MutA*) (Figure 7E). Furthermore, transient co-transfections of HEK293T cells with constructs carrying a *p63A-luciferase* reporter and β-*catenin*, resulted in a 5.5 fold-increase of *p63A* luciferase activity relative to an empty vector. In contrast, a construct carrying point mutations in the Lef1-Tcf motif within the *p63A* region (*p63MutA*) did not transactivate luciferase after co-transfection with β-*catenin* (Figure 7F). These

results demonstrated that Wnt effectors transactivate *p63* through a *p63A* regulatory region. Thus, *p63* is a midfacial target of Wnt in this mouse model.

Pbx-dependent Wnt-p63-Irf6 regulatory module in midfacial morphogenesis

Among mediators of apoptosis, the p53 family member p63 is known for its transcriptionally-regulated apoptotic activity (Pietsch et al., 2008; Rinne et al., 2007). *P63* deficiency results in various abnormalities including CL/P both in human and mouse (Rinne at al., 2007; Thomason et al., 2008). Notably, it was recently reported that the mouse *Irf6* gene is expressed in the epithelial seams of the λ (Rahimov et al., 2008) and is a target of p63 in palatal tissues. Indeed, p63 directly binds to a characterized orofacial enhancer (229 motif) within the *Irf6* locus (Rahimov et al., 2008; Thomason et al., 2010) (Figure 8A and 8B). Given these findings, we assessed *Irf6* expression in *Pbx* compound and *Wnt9b*$^{-/-}$ mutants and controls and found that *Irf6* was similarly down-regulated at λ in embryos from both mutant lines (Figure 8C–8H), placing *Irf6* within a regulatory module downstream of *Pbx* and *Wnt*. We then analyzed whether p63 directly binds to the 229 motif within the *Irf6* orofacial enhancer. ChIP-qPCR, on E11.0 facial process chromatin using two different Abs (4A4 and H129), showed *p63* enrichment at the *Irf6* orofacial enhancer (Figure 8I). Within the 229 motif, the p63 binding site is conserved only within mammals (Figure 8B). These results established an additional level of regulatory complexity within the described module at λ, whereby at the bottom of the cascade *Irf6* is a target of p63 in midfacial morphogenesis. The primary role of Pbx-directed Wnt signaling as a key determinant of midfacial morphogenesis within the delineated regulatory module was further demonstrated by complete rescue of the CL in five out of five *Pbx* compound mutants via ectopic expression of *Wnt1* in Crect-positive (Reid et al., 2011) SCE cells (Figure 8J–8L).

In summary, using our mouse model, we have established a Pbx-directed spatio-temporal regulatory module at λ, whereby *Pbx* directly controls midfacial Wnt through the W3 RE. In turn, Wnt effectors transactivate *p63*, which directly regulates *Irf6*, the mouse ortholog of *IRF6*, which is most commonly mutated in human CL/P (Dixon et al., 2011; Zucchero et al., 2004). Loss of multiple *Pbx* genes at λ disrupts the Wnt-p63-Irf6 regulatory module resulting in localized suppression of apoptotic programs and CL/P (Figure 8M).

Discussion

The face and its features best identify human beings and facilitate direct interpersonal communication and interaction. As a result, disfigured individuals often encounter severe hardship, due to lack of social acceptance because of their abnormal appearance. Among human craniofacial birth defects, CL/P and CPO are the most common anomalies. They require multiple cycles of surgery, speech therapy, orthodontics, and cause high morbidity in affected children; as such they have a significant social impact. Morphogenesis of the face requires TFs, signaling molecules, and effector proteins that are essential for tight coordination of cellular behaviors including migration, cells proliferation, differentiation, and apoptosis (Cox, 2004; Jiang et al., 2006). Perturbation of any of these processes result in facial abnormalities. As craniofacial development is similar in humans and mice (Gritli-Linde, 2008; Tamarine and Boyde, 1977), the mouse represents an ideal system to model craniofacial morphogenesis and its abnormalities.

Here we showed that *Pbx* genes (*Pbx1-2-3*) are highly expressed in the developing murine head with broader expression domains than those of *Hox* genes, in particular in the “Hox-less” face (Creuzet et al., 2005) and at the λ of the early embryo. *Pbx* homeoproteins are known as Hox cofactors for their interactions with 3’ Hox partners in target gene regulation during development (Moens and Selleri, 2006; Tumpel et al., 2009). However, the finding of fully penetrant CL/P in mice with compound *Pbx* loss in the *Hox*-less midfacial SCE

established Hox-independent functions of Pbx in facial morphogenesis. Additionally, the presence of CL/P only in *Pbx* compound mutants that lack both copies of *Pbx1* highlighted the preeminent role of *Pbx1* in midfacial morphogenesis and the collaborative, yet critical, roles of *Pbx2* and *Pbx3* in domains of co-expression. These results are in agreement with the primary requirement of *Pbx1* in skeletogenesis (Capellini et al., 2006 and 2010). Notably, in midfacial domains levels of *Pbx1* were found to be highest in comparison with those of the related family members. It was recently reported that *PBX1*, which is located on human chromosome 1q24, is linked to SNP rs12047510, a risk variant for CL/P (Beaty et al., 2010) and that the PBX dimerizing cofactor MEIS2 is deleted in a patient affected by midfacial clefting (Crowley et al., 2010). In our mouse model, CL/P was present only when multiple *Pbx* genes were lost simultaneously, suggesting that in humans multiple *PBX* genes or cofactors have to be concomitantly mutated to yield CL/P, consistent with the multigenic origin of human CL/P (Dixon et al., 2011).

Although they often occur together, CL/P and CPO differ in their etiology (Dixon et al., 2011). While multiple murine models of CPO are available, those for CL/P are sparse (Gritli-Linde, 2008); hence, our mouse lines offer unique reagents for modeling human CL/P. *Pbx1* SCE-specific inactivation, with either *Foxg1Cre* or *Crect* deleter mice, on a *Pbx2*- or *Pbx3*-deficient background, was sufficient to yield CL/P. In contrast, *Pbx1* inactivation in *Wnt1*-positive CNC-derived mesenchyme, on a *Pbx2*- or *Pbx3*-deficient background, did not generate CL/P, but resulted in CPO. Overall, these findings demonstrated a different etiology for murine CL/P and CPO, at least in regard to *Pbx* requirements in different tissues.

Components of the Wnt/β–catenin pathway (van Amerogen and Nusse, 2009) are conserved across species and are critical for multiple developmental processes, including face morphogenesis (Fossat et al., 2011). Indeed, they are expressed in chick and mouse midface (Brugmann et al., 2007; Lan et al., 2006; Reid et al 2011; Song et al., 2009) and Wnt signaling has an important role in species-specific facial patterning. Furthermore, loss-of-function of Wnt/β–catenin pathway components is associated with midfacial malformations and clefting (Carroll et al., 2005; Juriloff et al., 2006). In this study, we established a strong genetic interaction between *Pbx* and *Wnt9b* and demonstrated that Pbx homeoproteins directly control Wnt signaling, by binding to a *W3* RE that directs *Wnt* midfacial expression. An additional level of complexity within this network resides in the observed genetic control of *Fgf8* by *Pbx*. While *Fgf8* expression was diminished at *Pbx* mutant λ, direct regulation of *Fgf8* by Pbx was not found (data not shown), supporting indirect control of *Fgf8* by *Pbx*. These findings are in agreement with reports showing that *Fgf8* is a target of β–catenin in the head (Paek et al., 2011; Wang et al., 2011). In addition, we revealed that *Fgf8* does not act upstream of *Wnt9b*, excluding a cross-regulatory loop between these two genes in midface morphogenesis. Overall, this study established a genetic cascade wherein Pbx proteins regulate *Wnt9b*-*Wnt3*, which, in turn, indirectly control *Fgf8* in face morphogenesis (Figure 8M).

While at the *Pbx* mutant λ proliferation was not affected, apoptosis was absent. Indeed, wt embryos exhibited extensive epithelial cell death at λ, whereas the corresponding domains of *Pbx* compound mutants were devoid of apoptotic cells. Thus, our findings established that, in this mouse model, cellular epithelial removal from λ is partly controlled by programmed cell death via Pbx-dependent Wnt signaling. These results are consistent with loss of apoptosis reported in palatal and upper lip formation (He et al., 2011; Jiang et al., 2006; Song et al., 2009). Additionally, loss of apoptosis explained at least in part the persistence of epithelium at λ of *Pbx* compound mutants, whereby the epithelial seams are retained after coalescence of the midfacial prominences. Notably, in *Pbx* compound mutants, the high cellular levels of E-cadherin observed in the aberrant “bridge” at the λ may result from

altered Wnt signaling, since Lef1/β-catenin suppress E-cadherin expression in keratinocytes (Jamora et al., 2003). The delineated abnormal morphogenetic events at the mutant λ likely mediate the CL/P phenotype of *Pbx* compound mutants. Absence of detectable apoptosis at the *Pbx* mutant λ indicated that Pbx proteins act as apoptotic inducers in midfacial morphogenesis in this model. Interestingly, *p63* and *Irf6*, mediators of apoptosis in a few contexts (Ingraham et al., 2006; Pietsch, et al. 2007), are also expressed at λ during face development.

Analyses of *p63* mutant mice revealed that p63 is required for the formation and maintenance of a normal epidermal layer (Yang et al. 1999). Additionally, *p63* loss results in various abnormalities including CL/P (Thomason et al., 2010). The finding that p63 was absent from *Pbx* mutant λ and that therein Wnt controlled *p63* expression via binding of Lef-Tcf to a novel *p63* regulatory element, established p63 as an *in vivo* target of Wnt. Absence of apoptosis at the λ of *p63* mutants corroborated the molecular results, placing p63 as a downstream effector within the Pbx-Wnt regulatory module. Furthermore, it was recently reported that *p63* and *Irf6* interact epistatically in palatogenesis (Thomason et al., 2010). Our observation that *Irf6* was reduced at the λ of both *Pbx* and *Wnt9b* mutants and that p63 regulated *Irf6* expression via binding to an *Irf6* orofacial enhancer (Rahimov et al., 2008; Thomason et al., 2010), highlighted an additional level of regulatory complexity within the delineated module. Indeed, *Irf6* is a target of p63 in the midface and p63 acts as a cell-death inducer at λ preceding fusion of midfacial processes. In sum: dysregulation of the identified Pbx-dependent *Wnt-p63-Irf6* network, linking together multiple genes within a cascade at murine λ, is responsible for abnormal lip and primary palate formation in our mouse model and is consistent with the multigenic origin of human CL/P (Dixon et al., 2011).

The *W3* midfacial RE, which mediates *Wnt* regulation by Pbx, is evolutionarily conserved not just among mammals but throughout the amniotes. The IR sequences are not conserved in *Xenopus*, and are absent in stickleback and zebrafish, in which *Wnt9b* and *Wnt3* map to different chromosomes (Jezewski et al., 2008). Similarly, while the elements regulating *p63* and *Irf6* within the Pbx-controlled module are conserved in mammals, their conservation is lost in other amniotes, *Xenopus*, and fish. Notably, λ is absent in fish, but it is present in birds, reptiles, and mammals. In mammals, λ is developmentally and functionally more complex and critical for the morphogenesis and positioning of choanae, upper lip, primary and secondary palate (Compagnucci et al., 2011). Thus, it is conceivable that the Pbx-directed regulatory module at λ is an evolutionary innovation associated with the appearance of elaborate choanae and palate in mammals, all of which can be affected by CL/P (Mulvihill et al., 1980). Here, we showed that increased complexity of the regulatory module itself correlates with the gradual increase in complexity of λ and associated structures (choanae and palate), through evolutionary transitions from fish to tetrapodes to amniotes and to mammals. Overall, our findings clearly illustrate the importance of the lamdoidal junction in mammals. They further explain the high frequency of clefting phenotypes, due to the fact that mutations in any unit of the regulatory module at λ can result in CL/P.

In summary, we established a regulatory module at the midfacial λ, which is fully conserved within mammals, whereby *Pbx* direcly controls Wnt through an orofacial RE. The essential requirement of Pbx-directed Wnt signaling as an effector of midfacial morphogenesis was highlighted by complete rescue of the CL in *Pbx* mutants via ectopic expression of *Wnt1* in SCE, providing new approaches for tissue repair. Within the module, Wnt in turn transactivates *p63*, which directly regulates *Irf6*, the mouse ortholog of *IRF6*, the gene most commonly mutated in human non-syndromic CL/P. Overall, our study demonstrated that loss of multiple *Pbx* genes from midfacial SCE disrupts a *Wntp63-Irf6* regulatory network (Figure 8M), resulting in localized suppression of apoptotic programs and CL/P in this

mouse model. Identification of essential genes, midfacial enhancers, and mammalian regulatory modules, whose disruption yields CL/P, is a critical advance towards early diagnosis, prevention, and repair of this common birth defect.

Experimental Procedures

Scanning Electron Microscopy, Histological Analysis, Immunohistochemistry, Immunofluorescence, Whole-mount and Section *in situ* Hybridization, and Skeletal Preparations

See Supplemental Experimental Procedures.

mRNA Isolation and qRT-PCR

To obtain total RNA for gene expression analysis, dissected wt fnp tissues were harvested from E9.5 and E10.75 mouse embryos. Details in Supplemental Experimental Procedures.

Whole-Mount β-galactosidase Staining

Foxg1$^{Cre/+}$*;R26R-LacZ, Wnt1*$^{Cre/+}$*;R26R-LacZ,* and *BAT-gal* embryos were collected from E9.5 to E11.5 and stained for β-galactosidase as described (Rowitch et al., 1999).

Chromatin Immunoprecipitation (ChIP) Assay

150/200 wt fnp tissues were dissected in PBS/PMSF from E9.5–E11.5 embryos. Specimens were maintained in PBS+PMSF+AP (Complete Mini Roche) and kept on ice during dissection. After disrupting the tissues with a 20G syringe, crosslinking was performed with 1% formaldehyde at RT and stopped using glycine at a final concentration of 0.125 M. Chromatin was prepared as described (Vitobello et al., 2011) and sheared by sonication until DNA fragments reached an average length of 500–1000 bp. Samples were immunoprecipitated ON at 4°C with the following Abs (Santa Cruz): Pbx1/2/3 (C20 sc 888X); Pbx2 (G20 sc890X); Pbx3 (D17 sc891X); Prep1 (N15 sc6245X); Meis2 (N17 sc10600X); Hoxa1 (N20 sc17146X); Lef1 (N17 sc8591X); and rabbit IgG (Sigma). The immunopreciptated DNA was resuspended in 30 µl of TE. Regions within the *Wnt9b-Wnt3* conserved region (W3) and within the *p63* conserved intron (region A), containing the Pbx1 and Lef1 binding sites, respectively, were tested by PCR using primer pairs listed in Supplementary Procedures. The fragments highlighted as Out not bound by Pbx or Lef1 proteins, were located in non-conserved, non-coding regions and thus were used as negative controls. Chromatin precipitated with rabbit IgG was used as a control of immunoprecipitation specificity. For quantitative ChIP, enrichment of specific DNA fragments was analyzed by real time PCR, using the ABI Prism 7000 thermocycler and QuantiTect SYBR Green PCR master mix (Quiagen). Immunoprecipitated DNA amounts were obtained from a standard curve of input DNA and normalized to rabbit IgG immunoprecipitations. Fold enrichment was calculated after normalization to rabbit IgG. Cut-off value for positive binding was set at 4. Primer sequences are described in Supplementary Procedures.

Electrophoretic Mobility Shift Assay (EMSA)

EMSAs were performed as described (Ferretti el al., 2000) using *in vitro* translated proteins, or nuclear extracts purified from fnp tissues. Sequences of the oligonucleotides spanning putative *Pbx* binding sites within conserved regions of the *Wnt9b-Wnt3* DNA intergenic region (Katoh, 2005) used in EMSA are described in the text. Oligonucleotides spanning the putative *Lef-Tcf* binding site within the first conserved intron of *p63* (region A) are illustrated in Figure 7. Primers sequences are described in Supplementary Procedures.

Hsp68LacZ Transgenesis in Mice

1700 bp (Tg1) and 450 bp (Tg3) DNA fragments spanning the putative W3 RE within the *Wnt3-Wnt9b* IR (Katoh, 2005) were PCR amplified from mouse C57Bl/6 genomic DNA using proof-reading TAQ (PCR Supermix High Fidelity, Invitrogen). See details in Supplementary Procedures.

Proliferation and Cell Death Assays

For proliferation assays, cells in M phase were detected by IHC using the PhosphoHistone H3 Ab (PHH3, rabbit polyclonal, cat. 06–570, Upstate) (Song et al., 2009), followed by treatments with biotin-SP-conjugated goat anti-rabbit IgG secondary Ab and the ABC staining kit, and visualized by 3,3-diaminobenzidine as a substrate. Epithelial and mesenchymal cells were counted separately, as indicated in Figure S7. We drew a line of fixed length perpendicular to the tip of the mnp and lnp on photographed sections. We then drew a second line of fixed length perpendicular to the first and counted all the cells within the enclosed space for all slides analyzed. Proliferation rates were calculated by counting PHH3-positive cells over the total number of cells in 20 sections for each embryo. From 200 to 400 cells per section were counted. Data were calculated from three embryos per each genotype. Bars represent mean +/− s.e.m. For cell death assays anti-Cleaved Caspapse3 (Promega G7481) Ab (1:200) was used. Paraffin-embedded sections were microwaved in citrate buffer to permit antigen retrieval and treated as described for immunofluorescence in Supplementary Procedures.

In vitro Transcriptional Assays

HEK 293T were cultured in D-MEM supplemented with 10% fetal calf serum, 2 mM L-glutamine (Invitrogen), in humidified 5% CO_2. Transient transfections were performed using Polyethyleneimine (Polysciencies) following the manufacturer's protocol. The constructs used in this assay are described in Supplemental Experimental Procedures. Cells were transfected with different combinations of *p63A-luciferase* reporter, empty vector, and vector carrying stable β-catenin to activate Wnt signaling. A plasmid encoding *renilla* was used as a transfection control. Cells were lysed 48 hours after transfection and then assayed for luciferase activity using the Dual-Luciferase Reporter Assay System (Promega). Values were normalized for β-gal activity. Data are mean ± s.e.m. of three independent experiments done in triplicate.

Statistical Methods

Results are expressed as mean ± s.e.m. from triplicate qPCR reactions. Student's "t" test was used when appropriate.

Highlights

- *Pbx* genes promote midfacial morphogenesis via direct activation of *Wnt9b-Wnt3*
- A Pbx-Wnt-p63-Irf6 module induces apoptosis at the embryonic lambdoidal junction (λ)
- Disruption of the Pbx-Wnt-p63-Irf6 module, conserved in mammals, causes cleft lip
- Ectopic *Wnt1* expression can rescue genetically cleft lip in *Pbx* mutants

Supplementary Material

Refer to Web version on PubMed Central for supplementary material.

Acknowledgments

We are grateful to Drs. M. Lewandoski and T. Carroll for generously providing *Fgf8* hypomorph embryos, *Wnt9b*-deficient mice and *Rosa-Wnt1* mice, respectively. We also thank Dr. D. Kingsley for the *SfiHsp68LacZ* plasmid; Dr. B. Wang for proliferation assays; Drs. E. Lacy, A. Foley, T. Capellini, and D. Noden for important discussions; and Cyagen, Inc. for transgenic embryos. Work supported by Marie Curie Fellowship (OIF-CT-2005-022003) to E. Ferretti; grants from MRC UK (G0901539) to J. Dixon and M.J. Dixon; the Royal Society and King's College London to M.J. Depew; MOD (#6-FY03-071), NIH (RO1 HD43997, 2RO1 HD061403, and R21 DE18031), Cleft Palate Foundation, and Alice Bohmfalk Trust to L. Selleri. L. Selleri is an Hirschl Scholar.

References

Beaty TH, et al. A genome-wide association study of cleft lip with 2004 and without cleft palate identifies risk variants near MAFB and ABCA4. Nature Genetics. 2010; 42:525–529. [PubMed: 20436469]

Brugmann SA, Goodnough LH, Gregorieff A, Leucht P, ten Berge D, Fuerer C, Clevers H, Nusse R, Helms JA. Wnt signaling mediates regional specification in the vertebrate face. Development. 2007; 134:3283–3295. [PubMed: 17699607]

Capellini TD, Di Giacomo G, Salsi V, Brendolan A, Ferretti E, Srivastava D, Zappavigna V, Selleri L. Pbx1/Pbx2 requirement for distal limb patterning is mediated by the hierarchical control of Hox gene spatial distribution and Shh expression. Development. 2006; 133:2263–2273. [PubMed: 16672333]

Capellini TD, et al. Scapula development is governed by genetic interactions of Pbx1 with its family members and with Emx2 via their cooperative control of Alx1. Development. 2010; 137:2559–2569. [PubMed: 20627960]

Carroll TJ, Park JS, Hayashi S, Majumdar A, McMahon AP. Wnt9b plays a central role in the regulation of mesenchymal to epithelial transitions underlying organogenesis of the mammalian urogenital system. Dev. Cell. 2005; 9:283–292. [PubMed: 16054034]

Compagnucci C, Fish JL, Schwark M, Tarabykin V, Depew MJ. Pax6 regulates craniofacial form through its control of an essential cephalic ectodermal patterning center. Genesis. 2011; 49:307–325. [PubMed: 21309073]

Cox TC. Taking it to the max: the genetic and developmental mechanisms coordinating midfacial morphogenesis and dysmorphology. Clin. Genet. 2004; 65:163–176. [PubMed: 14756664]

Creuzet S, Couly G, Le Douarin NM. Patterning the neural crest derivatives during development of the vertebrate head: insights from avian studies. J. Anat. 2005; 207:447–459. [PubMed: 16313387]

Crowley MA, Conlin LK, Zackai EH, Deardorff MA, Thiel BD, Spinner NB. Further evidence for the possible role of MEIS2 in the development of cleft palate and cardiac septum. Am. J. Med. Genet. A. 2010; 152A:1326–1327. [PubMed: 20425846]

Depew MJ, Compagnucci C. Tweaking the hinge and caps: testing a model of the organization of jaws. J. Exp. Zool. B. Mol. Dev. Evol. 2008; 310:315–335. [PubMed: 18027841]

Dixon MJ, Marazita ML, Beaty TH, Murray JC. Cleft lip and palate: understanding genetic and environmental influences. Nat. Rev. Genet. 2011; 12:167–178. [PubMed: 21331089]

Ferretti E, Marshall H, Pöpperl H, Maconochie M, Krumlauf R, Blasi F. Segmental expression of Hoxb2 in r4 requires two separate sites that integrate cooperative interactions between Prep1, Pbx and Hox proteins. Development. 2000; 127:155–166. [PubMed: 10654609]

Fossat N, et al. Stringent requirement of a proper level of canonical WNT signalling activity for head formation in mouse embryo. Development. 2011; 138:667–676. [PubMed: 21228006]

Gritli-Linde A. The etiopathogenesis of cleft lip and cleft palate: usefulness and caveats of mouse models. Curr. Top. Dev. Biol. 2008; 84:37–138. [PubMed: 19186243]

He F, Xiong W, Wang Y, Li L, Liu C, Yamagami T, Taketo MM, Zhou C, Chen Y. Epithelial Wnt/β-catenin signaling regulates palatal shelf fusion through regulation of Tgfβ3 expression. Dev. Biol. 2011; 350:511–519. [PubMed: 21185284]

Hébert JM, McConnell SK. Targeting of cre to the Foxg1 (BF-1) locus mediates loxP recombination in the telencephalon and other developing head structures. Dev. Biol. 2000; 222:296–306. [PubMed: 10837119]

Ingraham CR, et al. Abnormal skin, limb and craniofacial morphogenesis in mice deficient for interferon regulatory factor 6 (Irf6). Nat. Genet. 2006; 38:1335–1340. [PubMed: 17041601]

Jamora C, DasGupta R, Kocieniewski P, Fuchs E. Links between signal transduction, transcription and adhesion in epithelial bud development. Nature. 2003; 422:317–322. [PubMed: 12646922]

Jezewski PA, Fang PK, Payne-Ferreira TL, Yelick PC. Zebrafish Wnt9b synteny and expression during first and second arch, heart, and pectoral fin bud morphogenesis. Zebrafish. 2008; 3:169–177. [PubMed: 18694329]

Jiang R, Bush JO, Lidral AC. Development of the upper lip: morphogenetic and molecular mechanisms. Dev. Dyn. 2006; 235:1152–1166. [PubMed: 16292776]

Juriloff DM, Harris MJ, McMahon AP, Carroll TJ, Lidral AC. Wnt9b is the mutated gene involved in multifactorial nonsyndromic cleft lip with or without cleft palate in A/WySn mice, as confirmed by a genetic complementation test. Birth. Defects. Res. A. Clin. Mol. Teratol. 2006; 76:574–579. [PubMed: 16998816]

Katoh M. Comparative genomics on Wnt3-Wnt9b gene cluster. Int. J. Mol. Med. 2005; 15:743–747. [PubMed: 15754041]

Kondo S, et al. Mutations in IRF6 cause Van der Woude and popliteal pterygium syndromes. Nat. Genet. 2002; 32:285–289. [PubMed: 12219090]

Lan Y, Ryan RC, Zhang Z, Bullard SA, Bush JO, Maltby KM, Lidral AC, Jiang R. Expression of Wnt9b and activation of canonical Wnt signaling during midfacial morphogenesis in mice. Dev. Dyn. 2006; 235:1448–1454. [PubMed: 16496313]

Liu W, Sun X, Braut A, Mishina Y, Behringer RR, Mina M, Martin JF. Distinct functions for Bmp signaling in lip and palate fusion in mice. Development. 2005; 132:1453–1461. [PubMed: 15716346]

Maretto S, et al. Mapping Wnt/beta-catenin signaling during mouse development and in colorectal tumors. Proc. Natl. Acad. Sci. U S A. 2003; 100:3299–3304. [PubMed: 12626757]

Meyers EN, Lewandoski M, Martin GR. An Fgf8 mutant allelic series generated by Cre- and Flp-mediated recombination. Nat. Genet. 1998; 18:136–141. [PubMed: 9462741]

Milunsky JM, et al. TFAP2A mutations result in branchio-oculo-facial syndrome. Am. J. Hum. Genet. 2008; 82:1171–1177. [PubMed: 18423521]

Moens CB, Selleri L. Hox cofactors in vertebrate development. Dev. Biol. 2006; 291:193–206. [PubMed: 16515781]

Mulvihill JJ, Mulvihill CG, Priester WA. Cleft palate in domestic animals: epidemiologic features. Teratology. 1980; 1:109–112. [PubMed: 7385051]

Niemann S, Zhao C, Pascu F, Stahl U, Aulepp U, Niswander L, Weber JL, Müller U. Homozygous *WNT3* Mutation Causes Tetra-Amelia in a Large Consanguineous Family. Am. J. Hum. Genet. 2004; 74:558–563. [PubMed: 14872406]

Noden DM, Trainor PA. Relations and interactions between cranial mesoderm and neural crest populations. J. Anat. 2005; 207:575–601. [PubMed: 16313393]

Paek H, Hwang JY, Zukin RS, Hébert JM. β-Catenin-Dependent FGF Signaling Sustains Cell Survival in the Anterior Embryonic Head by Countering Smad4. Dev Cell. 2011; 20:689–699. [PubMed: 21571225]

Pietsch EC, Sykes SM, McMahon SB, Murphy ME. The p53 family and programmed cell death. Oncogene. 2008; 27:6507–6521. [PubMed: 18955976]

Rahimov F, et al. Disruption of an AP2-alpha binding site in an IRF6 enhancer is associated with cleft lip. Nat. Genet. 2008; 11:1341–1347. [PubMed: 18836445]

Reid BS, Yang H, Melvin VS, Taketo MM, Williams T. Ectodermal WNT/β-catenin signaling shapes the mouse face. Dev. Biol. 2011; 349:261–269. [PubMed: 21087601]

Rhee JW, Arata A, Selleri L, Jacobs Y, Arata S, Onimaru H, Cleary ML. Pbx3 deficiency results in central hypoventilation. Am. J. Pathol. 2004; 165:1343–1350. [PubMed: 15466398]

Richardson RJ, Dixon J, Malhotra S, Hardman MJ, Knowles L, Boot-Handford RP, Shore P, Whitmarsh A, Dixon MJ. Irf6 is a key determinant of the keratinocyte proliferation-differentiation switch. Nat. Genet. 2006; 38:1329–1334. [PubMed: 17041603]

Riley BM, et al. Impaired FGF signaling contributes to cleft lip and palate. Proc. Natl. Acad. Sci. 2007; 104:4512–4517. [PubMed: 17360555]

Rinne T, Brunner HG, van Bokhoven H. p63-Associated Disorders. Cell Cycle. 2007; 6:262–268. [PubMed: 17224651]

Rowitch DH, S-Jacques B, Lee SM, Flax JD, Snyder EY, McMahon AP. Sonic hedgehog regulates proliferation and inhibits differentiation of CNS precursor cells. J. Neurosci. 1999; 19:8954–8965. [PubMed: 10516314]

Selleri L, et al. The TALE homeodomain protein Pbx2 is not essential for development and long-term survival. Mol. Cell. Biol. 2004; 24:5324–5331. [PubMed: 15169896]

Selleri L, Depew MJ, Jacobs Y, Chanda SK, Tsang KY, Cheah KS, Rubenstein JL, O'Gorman S, Cleary ML. Requirement for Pbx1 in skeletal patterning and programming chondrocyte proliferation and differentiation. Development. 2001; 128:3543–3547. [PubMed: 11566859]

Song L, et al. Lrp6-mediated canonical Wnt signaling is required for lip formation and fusion. Development. 2009; 136:3161–3171. [PubMed: 19700620]

Soriano P. Generalized lacZ expression with the ROSA26 Cre reporter strain. Nat. Genet. 1999; 21:70–71. [PubMed: 9916792]

Tamarine A, Boyde A. Facial and visceral arch development in the mouse embryo: a study by scanning electron microscopy. J. Anat. 1977; 124:563–580. [PubMed: 604328]

Thomason HA, Dixon MJ, Dixon J. Facial clefting in Tp63 deficient mice results from altered Bmp4, Fgf8 and Shh signaling. Dev. Biol. 2008; 321:273–282. [PubMed: 18634775]

Thomason HA, Zhou H, Kouwenhoven EN, Dotto GP, Restivo G, Nguyen BC, Little H, Dixon MJ, van Bokhoven H, Dixon J. Cooperation between the transcription factors p63 and IRF6 is essential to prevent cleft palate in mice. J. Clin. Invest. 2010; 120:1561–1569. [PubMed: 20424327]

Tümpel S, Wiedemann LM, Krumlauf R. Hox genes and segmentation of the vertebrate hindbrain. Curr. Top. Dev. Biol. 2009; 88:103–137. [PubMed: 19651303]

van Amerongen R, Nusse R. Towards an integrated view of Wnt signaling in development. Development. 2009; 136:3205–3214. [PubMed: 19736321]

Vitobello A, Ferretti E, Lampe X, Vilain N, Ducret S, Ori M, Spetzm JF, Selleri L, Rijli FM. Hox and Pbx Factors Control Retinoic Acid Synthesis during Hindbrain Segmentation. Dev. Cell. 2011; 20:469–482. [PubMed: 21497760]

Wang Y, Song L, Zhou CJ. The canonical Wnt/β-catenin signaling pathway regulates Fgf signaling for early facial development. Dev. Biol. 2011; 349:250–260. [PubMed: 21070765]

Yang A, et al. p63 is essential for regenerative proliferation in limb, craniofacial and epithelial development. Nature. 1999; 398:714–718. [PubMed: 10227294]

Zucchero TM, et al. Interferon regulatory factor 6 (IRF6) gene variants and the risk of isolated cleft lip or palate. N. Engl. J. Med. 2004; 351:769–780. [PubMed: 15317890]

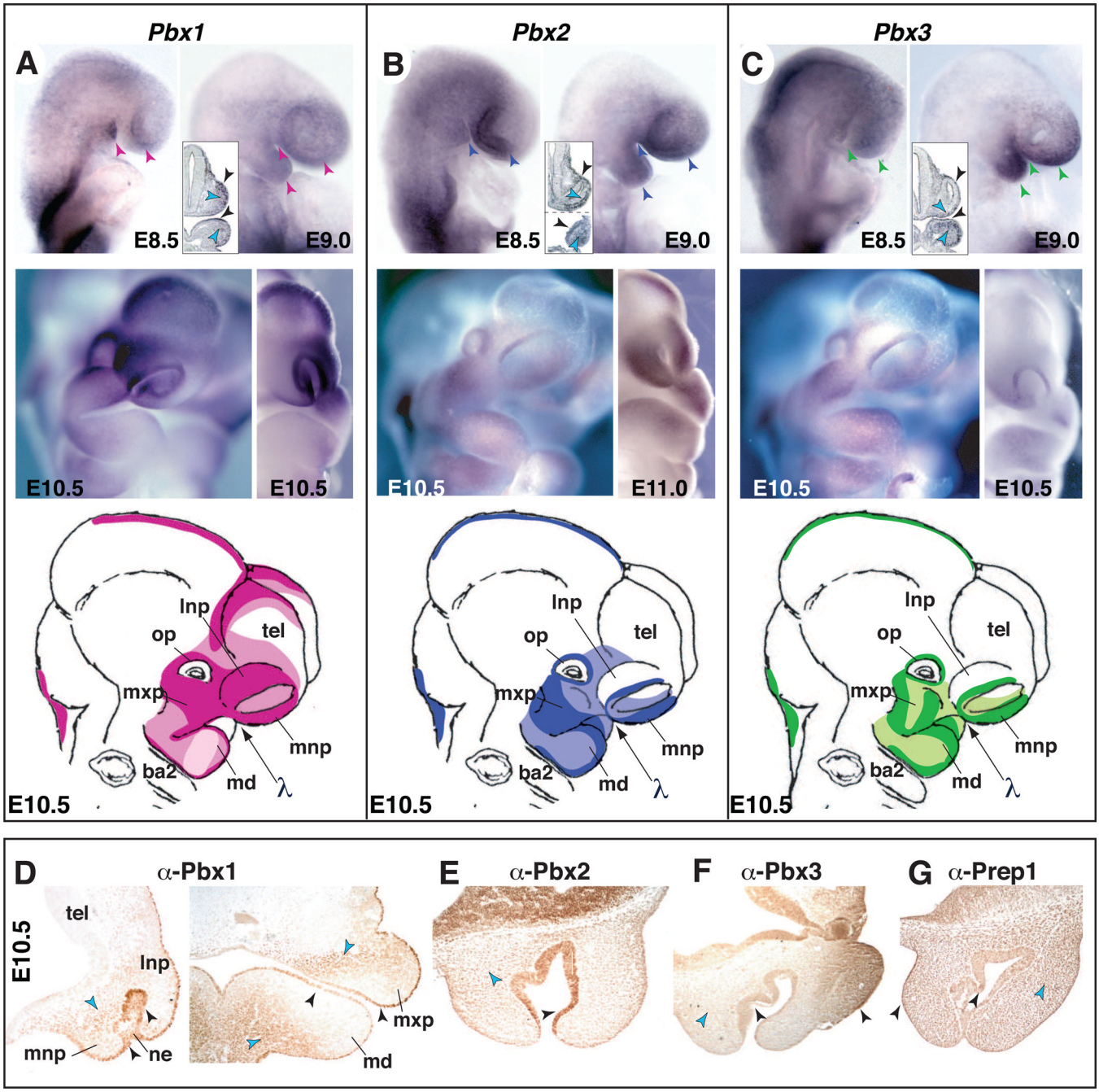

Figure 1. *Pbx1, Pbx2,* and *Pbx3* exhibit dynamic expression patterns during craniofacial development

(A–C) Whole-mount *in situ* hybridization (WISH) shows overlapping expression domains of *Pbx1* (A), *Pbx2* (B) and *Pbx3* (C) in E8.5 and E9.0 fnp. Insets: mRNA levels in E9.0 epithelium (black arrowheads) and mesenchyme (azure arrowheads). Marked expression of *Pbx* genes in E10.5 SCE and mesenchyme of mxp, lnp, and mnp. Lower panel: diagrams depicting unique and overlapping expression domains of *Pbx* genes in E10.5 heads. Hue saturation proportional to gene expression.

(D–G) Pbx proteins and their cofactor Prep1 in wt E10.5 fnp. Immunohistochemistry (IHC; coronal sections) reveals Pbx1 (D), Pbx2 (E), Pbx3 (F), and Prep1 (G) in epithelium of lnp

and mnp (black arrowheads) and in mesenchyme (azure arrowheads). Pbx1 is also detectable in epithelium of mxp and mandibular processes (md) (black arrowheads) and their proximal mesenchymal domains (azure arrows). Nasal Epithelium, ne; Optic Placode, op; Telenchepalon, tel. See also Figure S1 and Figure S2.

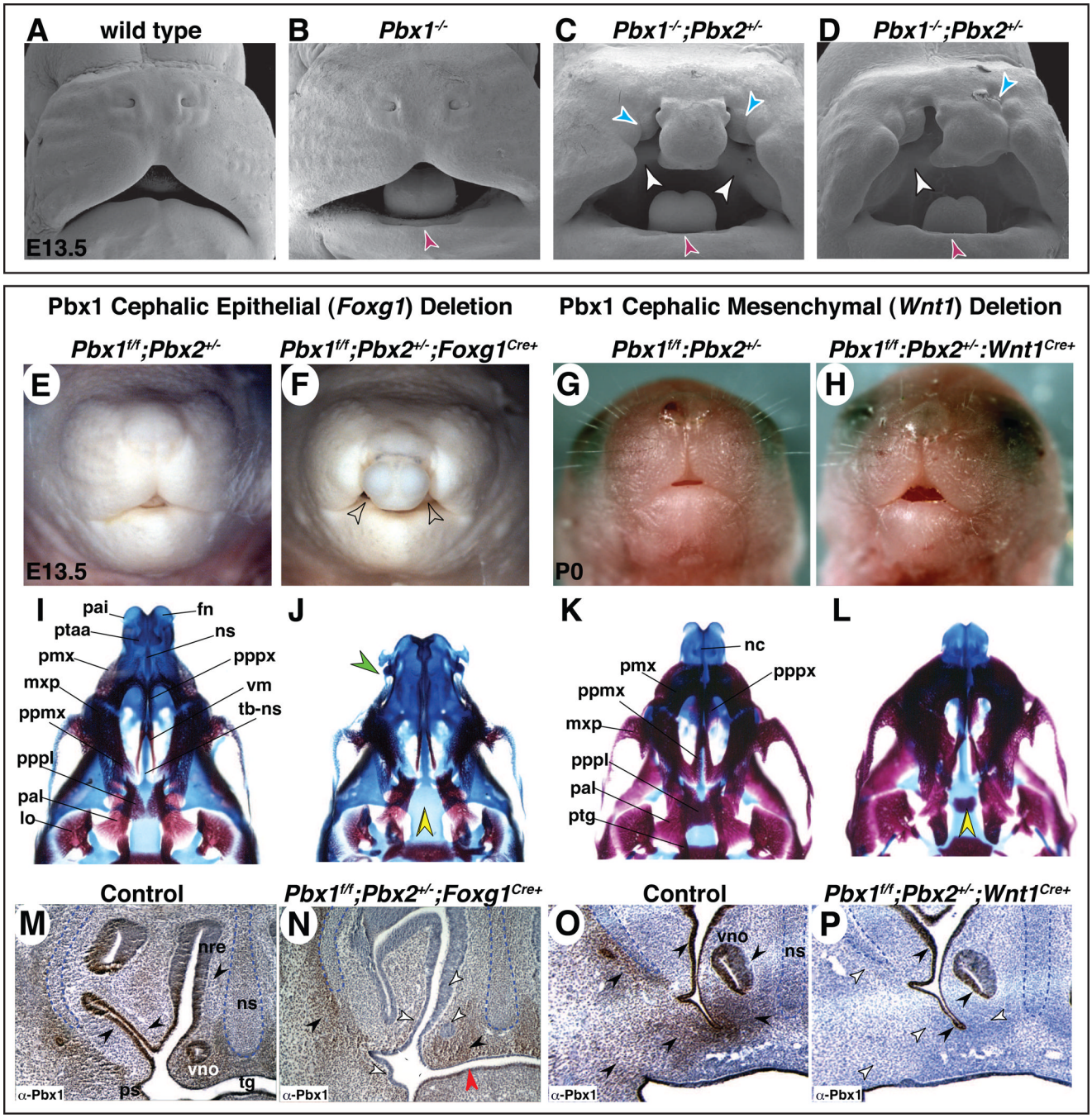

Figure 2. *Pbx* requirements in SCE for mifacial morphogenesis

(A–D) *Pbx* genes are required for midfacial and palate formation. Scanning Electron Microscopy (SEM) of E13.5 mouse embryos (frontal views): wt (A), $Pbx1^{-/-}$ (B) and $Pbx1^{-/-};Pbx2^{+/-}$ mutants (C,D). *Pbx1/2* mutants exhibit broader face, mandibular hypoplasia (pink arrowheads), CL (azure arrowheads), and CP (white arrowheads). (E–H) SCE-specific *Pbx1* inactivation (in *Foxg1*-positive cells) on a *Pbx2*-deficient background causes CL (E, F), while CNC-derived mesenchyme-specific *Pbx1* inactivation (in *Wnt1*-positive cells) does not (G, H).

(I–L) Ventral view of E17.5 $Pbx1^{f/f};Pbx2^{+/-};Foxg1^{Cre/+}$ skeletal preparation (J) shows CP (yellow arrowhead) and absence of premaxillae (green arrowhead) *versus* control (I).

Pbx1$^{f/f}$;*Pbx2*$^{+/-}$;*Wnt1*$^{Cre/+}$ newborn mouse shows CPO (yellow arrowhead) (L) *versus* control (K).

(M–P) Evaluation of Pbx1 loss by IHC of E13.5 *Pbx1*$^{f/f}$;*Pbx2*$^{+/-}$;*Foxg1*$^{Cre/+}$ and *Pbx1*$^{f/f}$;*Pbx2*$^{+/-}$;*Wnt1*$^{Cre/+}$ embryos reveals that in *Pbx1*$^{f/f}$;*Pbx2*$^{+/-}$;*Foxg1*$^{Cre/+}$ embryos (N) Cre-mediated Pbx1 loss occurs only in *Foxg1*-positive SCE (white arrowheads), while Pbx1 is maintained in tongue (tg) epithelium (red arrowhead), unlike in controls in which Pbx1 is present in both midfacial epithelium and mesenchyme (M, O) (black arrowheads). In *Pbx1*$^{f/f}$;*Pbx2*$^{+/-}$;*Wnt1*$^{Cre/+}$ embryos (P) Pbx1 is lost only from *Wnt1*-positive CNC-derived mesenchyme (white arrowheads), while it is maintained in SCE (black arrowheads). Lamina Obturans, lo; Nasal Capsule, nc; Nasal Septum, ns; Neuroepithelium, nre; Processus Alaris Inferioris, pai; Palatine, pal; Premaxilla, pmx; Palatal Process of Maxilla, ppmx; Palatal Process of Palatine, pppl; Palatal Process of Premaxilla, pppx; Palatal Shelf, ps; Processus Tranversus Anterior, ptaa; Pterygoid, ptg; Trabecular Plate-Nasal Septum, tb-ns; Vomer, vm; Vomero Nasal Organ, vno. See also Figure S3.

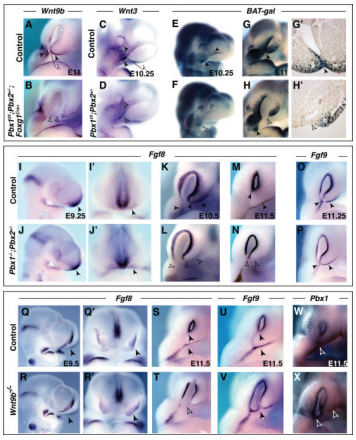

Figure 3. *Pbx* genes genetically regulate *Wnt9b*-*Wnt3*, which control *Fgf8* at the λ

(A–D) In controls *Wnt9b* (A) and *Wnt3* (C) are expressed in midfacial SCE (black arrowheads). In *Pbx* compound mutants, *Wnt9b* (B) and *Wnt3* (D) are down-regulated at λ (empty arrowheads).

(E–H') X-gal staining reveals high Wnt activity in midfacial SCE and λ of *Wnt*-reporter controls (black arrowheads) *versus* reduced or absent activity in *Pbx1/2* mutants (empty arrowheads). Section X-gal staining shows strong Wnt signaling at λ of E11 *Wnt*-reporter control (G') (black arrowhead), but not in *Pbx1/2* mutant littermates (H') (empty arrowhead).

(I–N) WISH reveals that *Fgf8* is unperturbed in E9.25 *Pbx1/2* midfacial SCE *versus* controls (I–J'; black arrowheads). *Fgf8* is present in epithelium of mnp and λ of E10.5 and E11.5 controls (K, M; respectively) (black arrowheads) and is reduced in *Pbx1/2* mutants (L, N; respectively) (empty arrowheads).

(O, P) *Fgf9* at λ is comparable in E11.5 control (O) and *Pbx1/2* mutant (P) (black arrowheads).

(Q–T) *Fgf8* is unperturbed in midfacial SCE of E9.25 *Wnt9b*$^{-/-}$ embryo (R, R') *versus* control (Q, Q') (black arrowheads), while it is down-regulated at λ of E11.5 *Wnt9b*$^{-/-}$ embryo (T) (empty arrowheads) *versus* control (S) (black arrowheads).

(U–V) *Fgf9* is unchanged at λ of E11.5 control (U) and *Wnt9b*$^{-/-}$ embryos (V) (black arrowheads).

(W–X) *Pbx1* is unperturbed at λ of *Wnt9b*$^{-/-}$ embryo (X) *versus* control (W) (black arrowheads). See also Figure S4 and Figure S5.

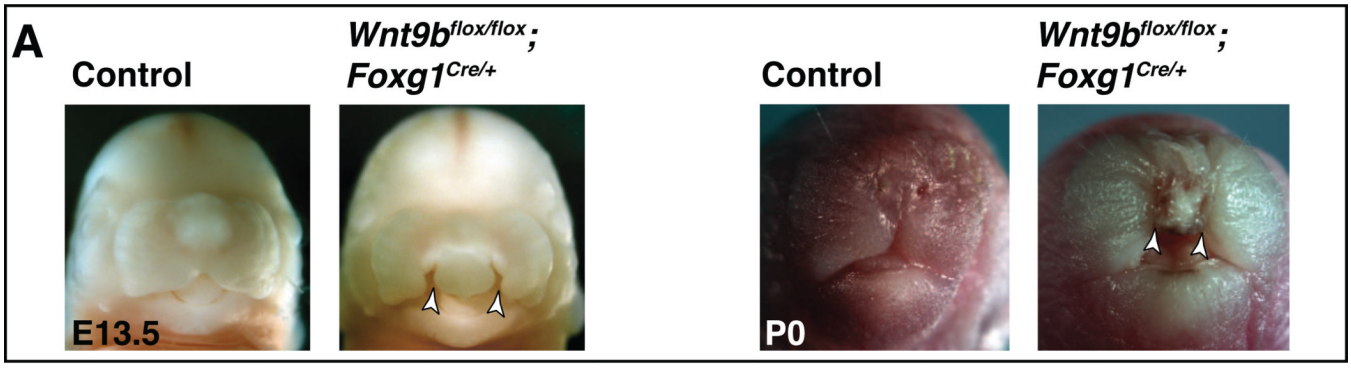

B

Genotype	Normal Lip (%)	Bilateral Cleft Lip (%)	Total (n)
Wnt9b$^{-/-}$	41.2	58.8	17
Wnt9b$^{-/-}$;*Pbx1*$^{+/-}$	0	100	12

Figure 4. Genetic interaction between *Pbx* and *Wnt9b*

(A) *Wnt9b* SCE-specific inactivation with the *Foxg1Cre* deleter results in CL/P, similarly to *Pbx1* SCE-specific inactivation on *Pbx2*-deficient background (in Figure 2F). *Wnt9b*$^{f/f}$;*Foxg1*$^{Cre/+}$ E13.5 embryos and P0 newborn mutants, respectively, exhibit bilateral CL (white arrowheads) and CP (not shown) *versus* their control littermates.

(B) Increase in frequency of CL in *Wnt9b*$^{-/-}$;*Pbx1*$^{+/-}$ compound mutants *versus* *Wnt9b*$^{-/-}$ single mutants. Distribution of CL in *Wnt9b*$^{-/-}$ and *Wnt9b*$^{-/-}$;*Pbx1*$^{+/-}$ compound mutants, respectively, is shown as a percentage of mutants that exhibit normal lip or bilateral CL over the total number of mutants analyzed.

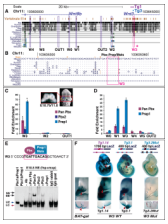

Figure 5. Pbx homeoproteins regulate *Wnt9b* and *Wnt3* by binding to a W3 RE in the midface

(A) Murine genomic organization of *Wnt9b-Wnt3* on chromosome 11, separated by a 24kb Intergenic Region (IR). Sequences conserved across vertebrates (Vertebrate El) indicated by brown boxes (UCSC Browser, mm9). Conserved regions W0–W2, W4, and W5 shown within purple boxes. Potential regulatory element W3 indicated within a pink box. All regions W0–W5 contain putative Pbx-Prep(Meis) binding sites. *Tg1* and *Tg3* highlight sequences within W3 used for transgenic constructs. Vertical blue bars represent discontinuity; green square brackets enclose short alignments that represent misalignment or transposon insertion; pale yellow box represents a gap in the sequence.

(B) Within W3, Pbx-Prep(Meis) binding site (within pink box) is conserved only within amniotes and not in amphibians and fish. Dots depict identical bases to reference; dashes indicate non-conserved sequences; white spaces absence of sequence.

(C–D) ChIP qPCR of immunoprecipitated chromatin from embryonic midfaces (shown in C, upper panel) reveals Pbx-Prep1 enrichment only at W1 and W3. Fold enrichment plotted over IgG. Specificity of Pbx and Prep1 recruitment at W1 and W3 tested by using non-specific primers (OUT1 and OUT2) located within non-conserved regions of the IR. Bars; mean +/− s.e.m. *<0.05.

(E) Upper panel: *W3* oligonucleotide sequence containing Pbx-Prep(Meis) binding site used for EMSA. The Pbx-Prep(Meis) binding site is indicated in bold and highlighted by pink box. Lower panel: EMSA with Nuclear Extracts (NE) from midfacial tissues and oligonucleotide *W3* reveals two DNA-binding complexes (UC, Upper Complex and LC, Lower Complex) consisting of Pbx and Prep(Meis) on *W3*. UC and LC comigrate with Pbx1a/Prep1 and Pbx1b-Prep1, respectively. Supershifted bands (SS) using Pbx Abs indicate that Pbx proteins bind to W3. Prep1 Ab inhibits complex formation.

(F) W3 drives *LacZ* expression in midfacial epithelium and λ of transgenic embryos. Upper panel: structures and concatamerization of *W3* transgenic constructs. Lateral and frontal views of E11.5 whole-mount X-gal stained *Tg1.14*, *Tg3.1* and *Tg3.2Mut* embryos. High expression of *LacZ* in *Tg1.14* and *Tg3.1* at λ (red arrowheads) and midface contrasts with lack of expression in *Tg3.2Mut* (white arrowhead). X-*gal* stained *Wnt*-reporter embryo (*BAT-gal*; left panel) reveals endogenous Wnt activity recapitulating *W3-LacZ* transgene expression in these domains. See also Figure S6.

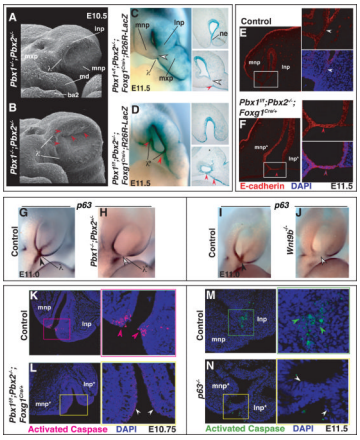

Figure 6. *Pbx*-dependent Wnt-*p63* cascade leads to localized suppression of apoptosis at λ of *Pbx* compound mutants

(A–B) SEM of *Pbx1/2* mutants (B) reveals enlarged and abnormal λ and nasal pit (red arrowheads) *versus* controls (A).

(C–D) SCE genetic fate mapping demonstrates that in controls midfacial epithelial seams fuse at λ, which is comprised of mesenchyme (white arrowhead), while in *Pbx1/2* mutant embryos they are maintained (red arrowheads).

(E–F) IF shows low E-cadherin in controls (E), indicating presence of mesenchyme (white arrowhead); conversely, high E-cadherin at the mutant λ (red arrowheads) points to epithelial persistence (F).

(G–J) *p63* is absent from both *Pbx1/2* mutant and *Wnt9b*$^{-/-}$ λ (H, J; empty arrowheads) *versus* respective controls (G, I; black arrowheads).

(K–N) Activated anti-caspase showing localized apoptosis, prior to epithelial seam fusion, at control λ (K) (pink arrowheads in inset) and absence of apoptosis at *Pbx* mutant λ (L) (white arrowheads in inset). Similarly, localized apoptosis is detected at control λ (M) (green arrowheads in inset), but not at *p63*$^{-/-}$ λ (N) (white arrowheads in inset). See also Figure S7.

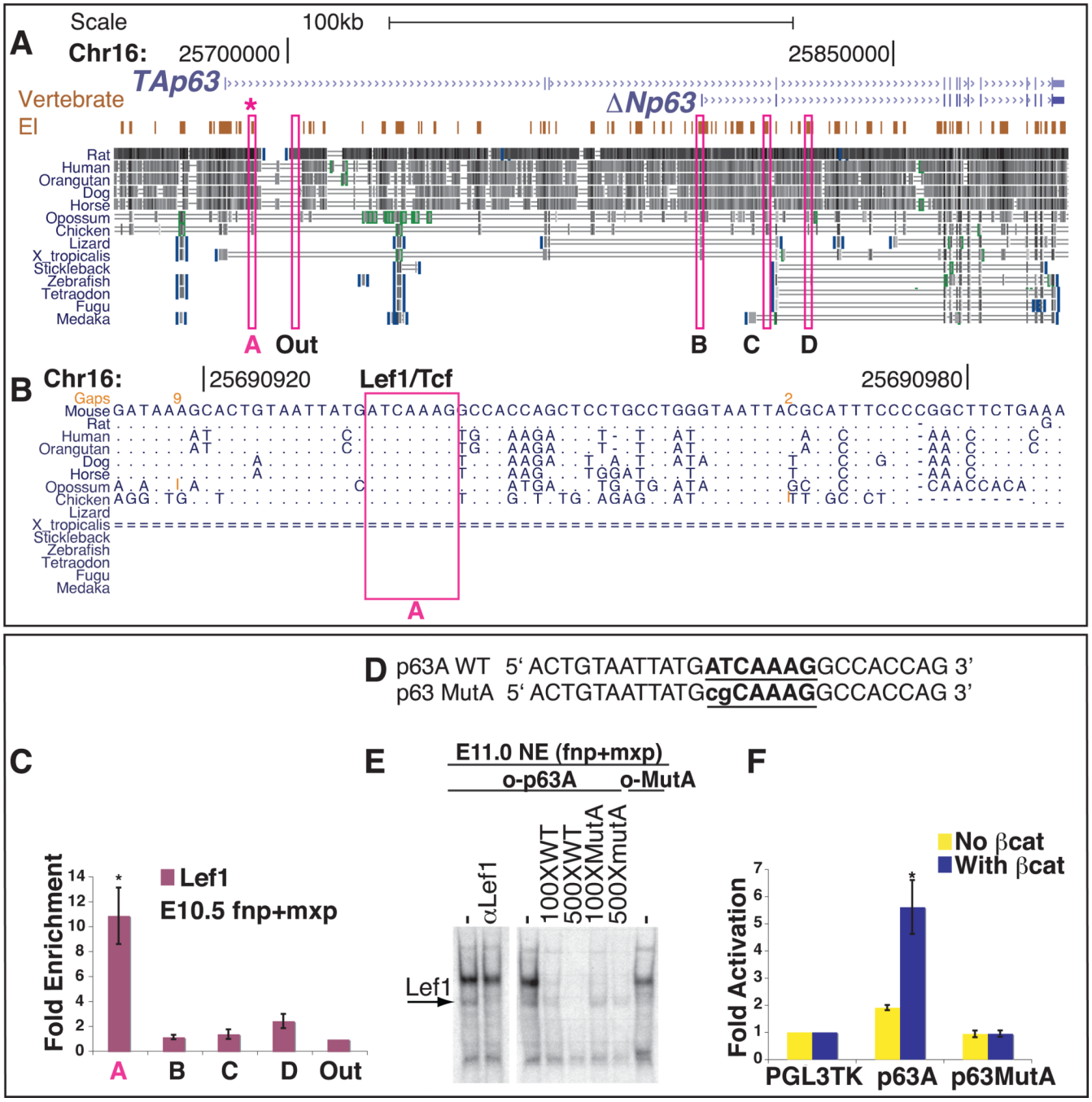

D p63A WT 5‘ ACTGTAATTATG**ATCAAAG**GCCACCAG 3’
p63 MutA 5‘ ACTGTAATTATG**cgCAAAG**GCCACCAG 3’

Figure 7. Recruitment of Lef1 to the *p63* locus in mouse embryonic midface

(A) Murine genomic organization of *p63* on chromosome 16. Conserved sequences across vertebrates (Vertebrate El) indicated by brown boxes (UCSC Browser, mm9). Potential regulatory elements containing putative Lef-Tcf binding sites highlighted by pink boxes and letters (A to D). Vertical blue bars represent discontinuity, and green square brackets enclose short alignments that represent misalignment or transposon insertion.

(B) The Lef1/Tcf binding site (pink box) within the *p63*A element (pink asterisk in A) is conserved within mammals and birds, but not in reptiles, amphibians, and fish. Dots: identical bases to reference. Dashes: non-conserved sequences. White spaces: absence of sequence.

(C) ChIP qPCR with Lef1 Abs and midfacial chromatin reveals Lef1 enrichment at *p63* element A (*p63A*), but at no other regions. Bars; mean ± s.e.m., *p<0.05.
(D) Oligonucleotide sequence containing wt (upper case, bold) and mutated (lower case, bold) Lef1/Tcf binding site.
(E) Retarded bands were detected by EMSA using nuclear extracts (NE) from E11.0 fnp and mxp of wt embryos and oligonucleotides p63A (o-p63A) and p63A mutated in the Lef1 binding site (o-MutA). Lef1 binding specificity was assessed using specific Abs against Lef1 (⟨Lef1), by which only one band was specifically competed (arrow). Competition assays (100- and 500-fold excess wt and mutated p63A oligonucleotide) show only one specific retarded band binding the Lef1 ATCAAAG site (arrow), which is competed increasingly by wt o-p63A, but not by o-MutA oligonucleotide. (−) above the lane indicates absence of Ab and competitor oligonucleotides.
(F) *p63A* enhances luciferase activity in the presence of β-catenin in transfected 293T cells. Transactivation is lost after Lef binding site mutagenesis (p63MutA). Bars; mean ± s.e.m., *p<0.05.

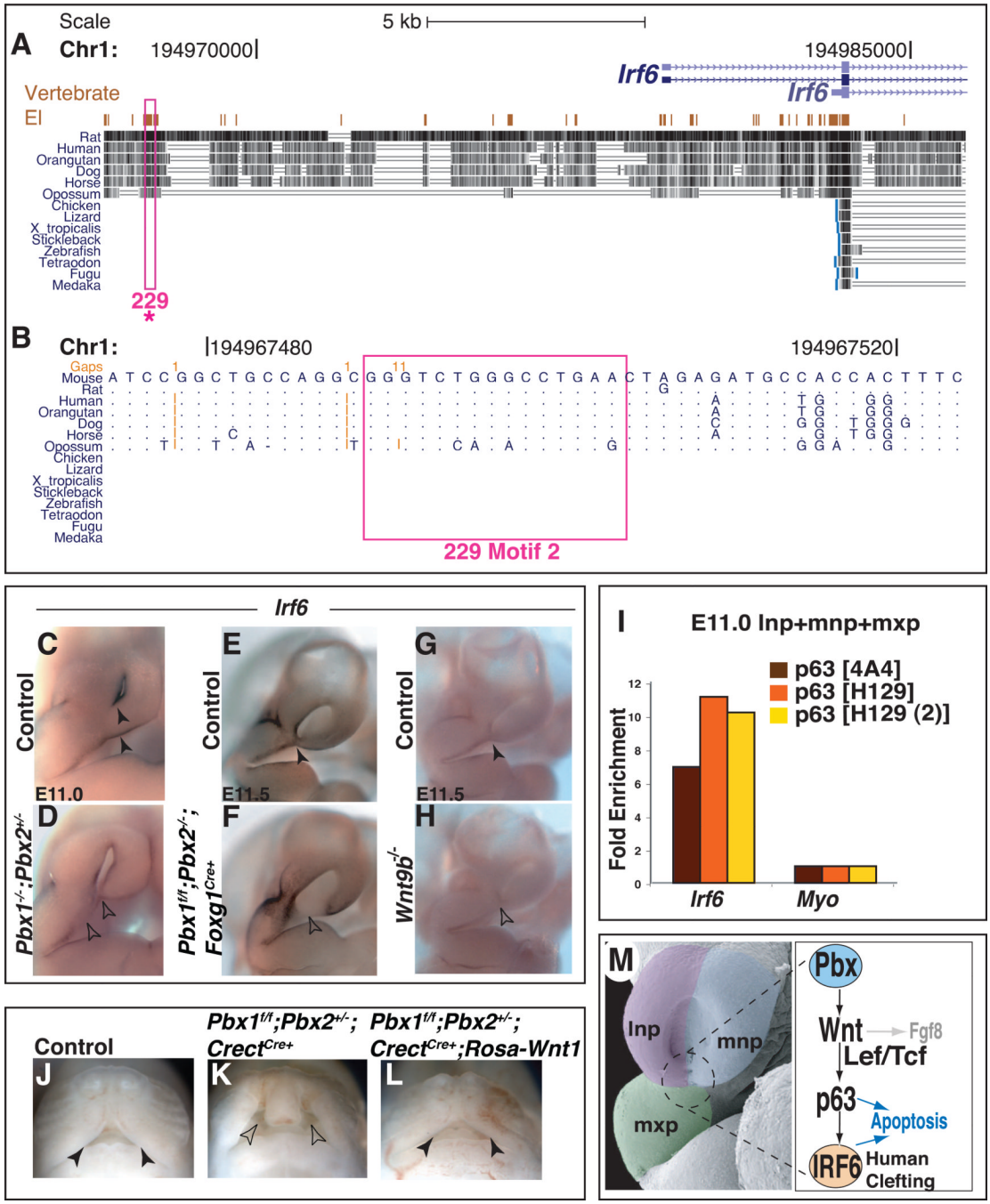

Figure 8. Pbx-directed Wnt-p63-Irf6 regulatory module at λ: a key determinant of midfacial morphogenesis

(A) Murine *Irf6* locus on chromosome 1 showing conserved sequences across vertebrates (Vertebrate El) indicated by brown boxes (UCSC Browser, mm9). The *Irf6 229* enhancer, within a pink box with asterisk, is conserved within mammals. Vertical blue bars represent discontinuity.

(B) Within the *229* enhancer, the p63 binding site (within pink box) is conserved only throughout mammals, but not in birds, reptiles, amphibians, and fish.

(C–H) *Irf6* is down-regulated (empty arrowheads) at λ of both *Pbx1/2* mutant and *Pbx1*$^{f/f}$*;Pbx2*$^{+/-}$*;Foxg1*$^{Cre/+}$ embryos (D, F) *versus* controls (C, E) (black arrowheads). *Irf6* is also lost at *Wnt9b*$^{-/-}$ λ (H) (empty arrowhead) *versus* control (G) (black arrowhead).
(I) ChIP-qPCR of p63 immunoprecipitated chromatin from mouse embryonic midface using two p63 Abs (4A4 and H129) reveals p63 binding to *Irf6* enhancer (Motif 229), but not to a control locus (*myoglobin*; *Myo*). Two independent experiments shown using H129 Ab (2).
(J–L) Complete rescue of the CL phenotype in *Pbx* mutant embryos via ectopic expression of *Wnt1* in Crect-positive SCE cells. Control and rescued lip (J, L) (black arrowheads); CL (K) (empty arrowheads).
(M) Model for Pbx essential role in midfacial morphogenesis. At λ (dashed circle), a Pbx-dependent *Wnt-p63-Irf6* regulatory module mediates apoptotic programs. Dysregulation of the module, which is fully conserved only within mammals, results in localized suppression of apoptosis and orofacial clefting.